ACS APPLIED MATERIALS & INTERFACES

RESEARCH ARTICLE

www.acsami.org

Antibiofouling Hybrid Dendritic Boltorn/Star PEG Thiol-ene Cross-Linked Networks

Jeremy W. Bartels,[†] Philip M. Imbesi,[‡] John A. Finlay,[§] Christopher Fidge,[‡] Jun Ma,[†] Jonathan E. Seppala,[⊥] Andreas M. Nystrom,[#] Michael E. Mackay,[⊥] James A. Callow,[§] Maureen E. Callow,[§] and Karen L. Wooley*[,‡]

[†]Department of Chemistry, Washington University in Saint Louis, One Brookings Drive, Saint Louis, Missouri 63130-4899, United States

[‡]Department of Chemistry, Texas A&M University, P.O. Box 30012, College Station, Texas 77842-3012, United States

[§]School of Biosciences, University of Birmingham, Birmingham B15 2TT, United Kingdom

[⊥]Materials Science & Engineering, University of Delaware, 201 Dupont Hall, Newark, Delaware 19716, United States

[#]Department of Neuroscience, The Swedish Medical Nanoscience Center, Karolinska Institutet, SE-177 76 Stockholm, Sweden

Supporting Information

ABSTRACT: A series of thiol-ene generated amphiphilic cross-linked networks was prepared by reaction of alkene-modified Boltorn polyesters (Boltorn-ene) with varying weight percent of 4-armed poly(ethylene glycol) (PEG) tetrathiol (0−25 wt %) and varying equivalents of pentaerythritol tetrakis(3-mercaptopropionate) (PETMP) (0−64 wt %). These materials were designed to present complex surface topographies and morphologies, with heterogeneity of surface composition and properties and robust mechanical properties, to serve as nontoxic antibiofouling coatings that are amenable to large-scale production for application in the marine environment. Therefore, a two-dimensional matrix of materials compositions was prepared to study the physical and mechanical properties, over which the compositions spanned from 0 to 25 wt % PEG tetrathiol and 0−64 wt % PETMP (the overall thiol/alkene (SH/ene) ratios ranged from 0.00 to 1.00 equiv), with both cross-linker weight percentages calculated with respect to the weight of Boltorn-ene. The Boltorn-ene components were prepared through the esterification of commercially available Boltorn H30 with 3-butenoic acid. The subsequent cross-linking of the Boltorn-PEG-PETMP films was monitored using IR spectroscopy, where it was found that near-complete consumption of both thiol and alkene groups occurred when the stoichiometry was ca. 48 wt % PETMP (0.75 equiv SH/ene, independent of PEG amount). The thermal properties of the films showed an increase in T_g with an increase in 4-armed PEG-tetrathiol wt %, regardless of the PETMP concentration. Investigation of the bulk mechanical properties in dry and wet states found that the Young's modulus was the greatest at 48 wt % PETMP (0.75 equiv of SH/ene). The ultimate tensile strength increased when PETMP was constant and the PEG concentration was increased. The Young's modulus was slightly lower for wet films at constant PEG or constant PETMP amounts, than for the dry samples. The nanoscopic surface features were probed using atomic force microscopy (AFM), where it was observed that the surface of the amphiphilic films became increasingly rough with increasing PEG wt %. On the basis of the physicochemical data from the diverse sample matrix, a focused compositional profile was then investigated further to determine the antifouling performance of the cross-linked Boltorn-PEG-PETMP networks. For these studies, a low, constant PETMP concentration of 16 wt % was maintained with variation in the PEG wt % (0−35 wt %). Antifouling and fouling-release activities were tested against the marine alga *Ulva*. Spore settlement densities were low on these films, compared to that on standards of polydimethylsiloxane and glass.

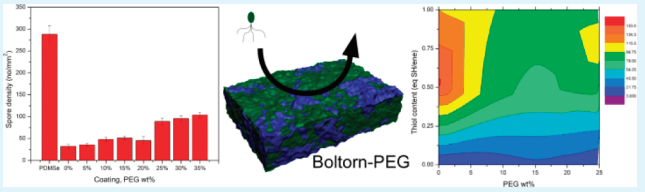

KEYWORDS: thiol-ene, cross-linking, Boltorn, poly(ethylene glycol), marine fouling, *Ulva*

INTRODUCTION

Over the past decade, there have been increased efforts to devise nonbiocidal coatings that inhibit the adhesion and/or promote the detachment of marine organisms on the hulls of ships and underwater structures. Biocidal metal-based paints, such as those containing tributyltin, are banned for maritime application, and copper oxide formulations, which are currently in use, are showing accumulation that may be irreversibly detrimental to the environment.[1−3] Recent efforts toward nontoxic, antifouling coatings have explored fluoropolymers,[4−8] silicone elastomers,[9−12] xerogels,[13] zwitterionic polymers,[14−16] and PEGylated polymers,[4−8,17−19] among others.[20−24] The surface and bulk properties of antifouling coatings, including the surface free energy,[25] elastic modulus,[26] wettability,[27] and roughness,[27−29] impact the ability of marine organisms to settle and attach. It is anticipated that a combination of these factors, giving the polymer coating a high degree of complexity,[5] are

Received: March 17, 2011
Accepted: May 23, 2011
Published: June 06, 2011

needed to combat the various mechanisms that are used by fouling organisms for settlement and adhesion to substrates.

Recent advances in polymer networks prepared by thiol−ene UV photopolymerization methods[30−33] have many attractive properties that can provide a high extent of compositional and surface complexities, giving potential promise for antifouling applications. Thiol-ene chemistry, used industrially since the 1970s,[34,35] has emerged as a facile "click" reaction that has been used to conjugate small molecules to polymers[36,37] and proteins,[38] and has been used to build complex nanostructures, such as dendrimers[30] and star polymers.[39] The thiol-ene process is attractive for making bulk films because it is insensitive to oxygen,[40] gives low shrinkage,[41] imparts high thermal stability, and proceeds to relatively high conversion, while being conducted at a rate that is as rapid as traditional UV cross-linking.[42−44] The thioether bonds in the cross-linked networks impart enhanced mechanical properties and provide chemical insensitivity to the final products.[42] Bulk thiol-ene cross-linking has been used for nanoimprint lithographic patterns,[45,46] inks,[47] adhesives[48] and biomaterials.[19,49] In addition to the many examples of traditionally UV-photocured films that have been reported as antifouling materials,[50,51] thiol-ene generated polymer networks are beginning to emerge as marine antifouling coatings.[50−52] With the breadth of chemical compatibilities that can be tolerated for components cross-linked via photoinitiated thiol−ene reactions, we were interested in further exploration of this chemistry for the preparation of nontoxic antifouling coatings, comprising the types of mixtures of small molecules and polymers that are expected to create high degrees of physical and chemical complexities for advanced antifouling performance.

Previous studies by our laboratory into coatings comprising hyperbranched fluoropolymers cross-linked with poly(ethylene glycol), (HBFP-PEG),[5] have led to the examination of antifouling materials with optimization of the chemistries used for their production and investigation of alternate components, in particular, replacement of the hyperbranched fluoropolymer. HBFP-PEG demonstrated unique antifouling properties,[5,6,53] uncommon mechanical behavior,[54,55] and interesting host−guest interactions with small organic molecules.[56] The HBFP-PEG mode of action for biofouling prevention is believed to be derived from a combination of complex surface topographies, morphologies, and compositions over nano- and microscopic dimensions. There are questions, however, about whether the fluorocarbon character is required for the properties of the HBFP-PEG. In addition, these coatings are derived from expensive reagents, are difficult to synthesize, lack optical translucence and require long periods of time to cure. Therefore, exploration into thiol-ene based networks that are comprised of alternate hyperbranched polymer materials was conducted to develop PEGylated coatings with affordable, commercially available precursors that cross-link rapidly and yield coatings of high degrees of optical transparency, without compromising tensile strength and surface complexity observed in the HBFP-PEG materials. Boltorn polymers[43] have been shown to undergo thiol-ene-based cross-linking[32,33,57] to provide uniformity throughout the networks, giving enhanced mechanical properties, narrow T_g's,[58] and increased thermal stabilities.[32] To be incorporated into networks via thiol-ene cross-linking, the large number of hydroxyl chain ends of dendritic Boltorn polyols, dendronized versions of poly(2,2-bis-(hydroxymethyl)propionic acid),[43] can be readily esterified to form either thiol-functionalized[57,59] or alkene-functionalized[32,60,61] macromolecules. Therefore, a highly branched, alkenylated Boltorn H30 polymer was chosen as the substitute for the HBFP component of HBFP-PEG, with cross-linking performed together with a 4-arm thiol-modified PEG and a tetra-thiol small molecule to assist with mechanical properties.

In this work, the Boltorn H30 polyol was per-enylated using simple esterification chemistry to yield Boltorn-ene, which was subsequently photo-cross-linked in a two-dimensional array that was designed to probe the physicochemical properties of the materials. Variations in the weight percent of 10 kDa 4-armed PEG tetrathiol (0, 5, 15, and 25 wt %, relative to Boltorn-ene) and pentaerythritol tetrakis(3-mercaptopropionate) (PETMP) small molecule cross-linker (0, 16, 32, 48, and 64 wt %, relative to Boltorn-ene) were employed to give variations in the thiol-to-alkene ratios (0.00, 0.25, 0.50, 0.75, and 1.00 equiv SH/ene). Reaction completion was monitored via IR spectroscopy. The coating surface and bulk properties were characterized by atomic force microscopy, contact angle, tensile strength, and thermal analysis experiments. Additionally, a comprehensive antifouling study was performed using the alga *Ulva* on Boltorn-PEG-PETMP coatings across a wider range of PEG wt % (0−35 wt %), while holding constant the PETMP.

EXPERIMENTAL SECTION

Instrumentation. Infrared spectra were obtained from a Perkin−Elmer Spectrum BX FTIR system as neat films on NaCl plates.

^{1}H NMR (300 MHz) and ^{13}C NMR (75 MHz) spectra were recorded on a Varian Mercury 300 MHz spectrometer using the solvent as an internal reference.

Gel permeation chromatography was performed on a Waters Chromatography, Inc. (Milford, MA), 1515 isocratic HPLC pump equipped with an inline degasser, a model PD2020 dual-angle (15° and 90°) light scattering detector (Precision Detectors, Inc.), a model 2414 differential refractometer (Waters, Inc.), and four PL_{gel} polystyrene-*co*-divinylbenzene gel columns (Polymer Laboratories, Inc.) connected in series: 5 μm Guard (50 × 7.5 mm), 5 μm Mixed C (300 × 7.5 mm), 5 μm 10^4 (300 × 7.5 mm), and 5 μm 500 Å (300 × 7.5 mm) using the Breeze (version 3.30, Waters, Inc.) software. The instrument was operated at 35 °C with THF as the eluent (flow rate set to 1.00 mL/min). Polymer solutions were prepared at a known concentration (ca. 3 mg/mL) and an injection volume of 200 μL was used. Data collection was performed with Precision Acquire 32 Acquisition program (Precision Detectors, Inc.) and analyses were carried out using Discovery32 software (Precision Detectors, Inc.) with a system calibration curve generated from plotting molecular weight as a function of retention time for a series of broad polydispersity poly(styrene) standards. .

UV cross-linking was performed by a single passing of pregel coated microscope slides through a Fusion UV 300S conveyor system equipped with a H bulb (300 W/inch) at a speed of 1 m/min.

Glass transition temperatures (T_g) were measured by differential scanning calorimetry (DSC) on a Mettler-Toledo DSC822^e (Mettler-Toledo, Inc., Columbus, OH), with a heating rate of 10 °C/min. Measurements were analyzed using Mettler-Toledo Star SW 7.01 software. The T_g was taken as the midpoint of the inflection tangent, upon the third heating scan.

Thermogravimetric analysis was performed under N_2 atmosphere using a Mettler-Toledo model TGA/SDTA851^e, with a heating rate of 5 °C/min. Measurements were analyzed using Mettler-Toledo Star SW 7.01 software.

In order to provide additional information into the surface thiol concentration remaining in the Boltorn-PEG-PETMP coatings postcross-linking, an experiment was devised wherein a 1.5 mM solution of the pro-fluorescent molecule, *N*-(7-dimethylamino-4-methylcoumarin-3-yl)

maleimide (DACM) in 10 mM pH 7.4 buffer with a minimum amount of DMF, was pipetted onto the Boltorn-PEG-PETMP coatings and allowed to sit for 2 h. The coatings were then washed extensively in deionized water, dried, and then imaged using fluorescence microscopy. Optical microscopy was performed on an Nikon Eclipse E200 microscope (Nikon Corp., Tokyo, Japan) under bright-field conditions, and images were collected with a Nikon D-500 digital camera at 4× objective, 1/15 exposure time and ISO 1600. The fluorescence was generated using a Semrock Brightline Calcofluor White Filter cube (CFW-BP01-Clinical-NTE) with an absorbance of 350 nm and emission of 440 nm. The fluorescence properties of DACM are Abs/Em 383/463 nm. Control images were digitally subtracted from the fluorescent images using ImageJ software (NIST).

Tapping-mode AFM measurements were conducted in air with an Asylum MFP-3D Stand Alone AFM(Asylum Research, Santa Barbara, CA) operated under ambient conditions with standard silicon tips [Vista Probes, T190−25; length (L), 225 μm; normal spring constant, 48 N/m; resonant frequency, 190 kHz].

Contact angles were measured as static contact angles using the sessile drop technique[62] with a Tantec CAM microcontact-angle meter and the half an gle measuring method. Advancing and receding contact angles (θ_a and θ_r) of 18 MΩ cm^{-1} nanopure water were measured on the films by placing a 2 μL drop on the surface, then increasing or decreasing the drop size by 1 μL, respectively. Time-dependent changes in the contact angles were measured over three hours in a similar manner, however, the coating was submerged in nanopure water between collection of data points and the surface was quickly dried with a Kimwipe prior to measurement. The reported values are an average of five such measurements on different regions of the same sample.

Elemental analysis was performed by Midwest Microlabs, LLC (Indianapolis, IN).

Tensile tests were performed on the Boltorn-PEG-PETMP series based upon a method adapted from ASTM D882−95a and conducted using a Rheometrics Solids Analyzer, RSA III (TA Instruments, New Castle, DE), at 22 °C and a Hencky strain of 0.01 s^{-1} with an initial grip separation of ∼5 mm. For each sample: (1) at least five dry specimens (dimensions: 10 mm × 5 mm × 0.5 − 1.0 mm) were tested; (2) three preswollen specimens (incubation time: >7 d) were tested in an RSA III Immersion Fixture filled with artificial seawater. Only samples in the "C" and "2" series (C1, C2, C3, C4, C5 and A2, B2, C2, D2) were tested wet. The tensile modulus (E_{dry} or E_{wet}, MPa) was calculated as the slope of the initial linear (Hookean) portion of the stress−strain curve, and the ultimate tensile strength (σ_{UTS}, MPa) and strain to failure (ε_f, %) were also recorded.

Materials. 3-Butenoic acid (97%), pentaerythritol tetrakis (3-mercaptopropionate) (PETMP, 97%), 1-hydroxycyclohexylphenyl ketone (99%), vinyltrimethoxysilane (vinyl-TMS, 98%), *N*-(7-dimethylamino-4-methylcoumarin-3-yl) maleimide (98%), 1,4-dioxane (99%), dichloromethane (99%), magnesium sulfate (anhydrous, *ReagentPlus*, ≥99.5%), and toluene (99.8% anhydrous) were obtained from Sigma-Aldrich, Inc. (St. Louis, MO) and were used as received. 4-armed PEG tetrathiol (10,000 Da) was obtained from Laysan Biochem. Boltorn H30 was kindly supplied by Perstorp. Chloroform-*d* (D, 99.8%) and *d*-MeOH (D, 99.8%) were obtained from Cambridge Isotope Laboratories. 4(Dimethylamino)pyridinium 4-toluenesulfonate (DPTS) was prepared using standard literature procedures.[63,64] Vinyl-trimethoxysilane-modified glass slides were prepared by submerging fresh microscope slides in a 5 v/v% solution of vinyl-TMS in anhydrous toluene for one hour, followed by copious rinsing with toluene. Argon ultrahigh purity grade gas (99.999%) was used as received from Praxair (St. Louis, MO). Coralife Scientific grade Marine Salt that was used for the preparation of artificial seawater was mixed according to directions from the manufacturer.

Boltorn-ene (1). 30.001 g of Boltorn H30 (8.57 × 10^{-3} mol, 1.0 equiv) was added to a 500 mL round-bottom flask equipped with a Teflon-coated stir bar. Toluene (100 mL) was added to the flask, which was fitted with a distillation apparatus, and contents were heated at reflux for an hour to ensure that the polymer was dissolved while residual water was removed via azeotropic distillation. DPTS (6.665 g, 2.26 × 10^{-2} mol, 10 wt %) and 3-butenoic acid (38.758 g, 4.50 × 10^{-1} mol, 1.6 equiv of COOH per Boltorn-OH) were added to the flask, which was then equipped with a condenser and allowed to heat at reflux at a high stir rate for 2 days. After the reaction was complete and slightly cooled, 300 mL of water was added to the mixture and the product was extracted against DCM (3 × 150 mL). The organic layer was dried over anhydrous $MgSO_4$ and then concentrated, yielding 44.1 g of a transparent, thick oil (90% yield). ^{1}H NMR spectroscopy showed quantitative conversion. The oil was stored at 4 °C to prevent side-reaction of the alkene groups. M_n^{NMR} = 5700 Da, M_w^{GPC} = 4800 Da (polystyrene equivalent), M_n^{GPC} = 2800 Da (polystyrene equivalent), M_w/M_n = 1.69. T_g = −37 °C. T_{decomp}: 427 °C, 94% mass loss. IR = 2944, 2882, 1736, 1650, 1564, 1470, 1222, 1126, 1010, 814, 684, 570 cm^{-1}. ^{1}H NMR (300 MHz, $CDCl_3$, ppm): δ 6.0−5.8 (br, —C*H*=CH$_2$, 5.2−5.1 (br, =C*H*$_2$, 4.4−4.1 (br, peripheral —C*H*$_2$−C(O)−), 3.8−3.5 (br, internal —C*H*$_2$−O-C(O)), 3.2−3.1 (br, —C*H*$_2$−CH═CH$_2$, 1.3−1.1 (br, multiplet −C*H*$_3$). ^{13}C NMR (75 MHz, $CDCl_3$, ppm): δ 206.4, 173.4, 172.2, 170.8, 139.6, 130.6, 128.7, 126.2, 118.5, 107.2, 65.5, 48.8, 46.8, 39.9, 38.7, 25.7, 21.1, 17.7. Elemental anal.: C, 57.21%; H, 6.51%.

Boltorn-PEG-PETMP Film Production. An array of Boltorn-PEG-PETMP networks were prepared at varying PEG wt % (0, 5, 15, and 25 w/w% of Boltorn-ene, corresponding to A, B, C, and D, respectively) and PETMP concentrations (0, 0.25, 0.50, 0.75, and 1.0 equiv of SH/ene, corresponding to 1, 2, 3, 4, and 5, respectively). For example, film C3 refers to a cross-linked film with 15 wt % PEG and 0.50 eq SH/ene PETMP concentration (32 wt %). The "SH" refers to thiols in the PETMP cross-linker and not from the PEG-tetrathiol, which are negligible in comparison. The photoinitiator 1-hydroxycyclohexylphenyl ketone was added as 5 w/w% of total solids to all samples. An example experimental is listed below and the remaining experimental can be found in the Supporting Information.

Preparation of Boltorn-PEG-PETMP film ***C3***. Boltorn-ene (3.494 g, 6.13 × 10^{-4} mol) was combined with 4-armed PEG tetrathiol (0.526 g, 5.23 × 10^{-5} mol), PETMP (1.110 g, 2.27 × 10^{-3} mol) and 1-hydroxycyclohexylphenyl ketone (0.245 g, 1.20 × 10^{-3} mol) in a scintillation vial. The vial was charged with 24.0 mL of 1,4-dioxane and the contents were vortexed until homogeneous. The contents were then syringed 1 mL/slide onto vinyl-TMS-modified glass slides and allowed to evaporate over a 20 min period, producing a thick pregel on the surface of the glass slide. The coated slides were then passed through the Fusion UV 300S conveyor system. T_g = −4 °C. T_{decomp}: 378 °C, 97% mass loss. IR = 3478, 3082, 2938, 1738, 1642, 1466, 1246, 1136, 1008, 872, 764, 614 cm^{-1}. Elemental anal.: C, 53.68%; H, 6.39%; S, 6.04%. Contact angle: Advancing (θ_a) = 86 ± 3°, receding (θ_r) = 69 ± 3°, hysteresis =17°.

Antifouling Boltorn-PEG-PETMP Film Production. A series of eight films were prepared for antifouling tests. The synthesis is similar to that of the previous Boltorn-PEG-PETMP films, but the films were prepared at a constant 0.25 eq SH/ene PETMP concentration (16 wt %) at varying PEG wt % (0, 5, 10, 15, 20, 25, 30, and 35 wt %) producing films AF0, AF5, AF10, AF15, AF20, AF25, AF30, and AF35, respectively.

Biofouling Assays. *Leaching.* Coatings were supplied in nanopure deionized water from which they were transferred to seawater 24 h before the start of the experiment. The slides remained wet and fully hydrated throughout the process.

Settlement of Spores. Reproductive tissue from *Ulva linza* was collected from Llantwit Major, Wales (51840′N; 3848′W). Zoospores released from the seaweed were diluted with seawater to produce a zoospore suspension of 1.0 × 10^6 zoospores mL^{-1} using the method of Callow, et al.[65] A suspension of zoospores (10 mL containing 1.0 × 10^6 spores mL^{-1}) was added to individual

Scheme 1. Esterification of Boltorn H30 with 3-Butenoic Acid to Produce Boltorn-ene

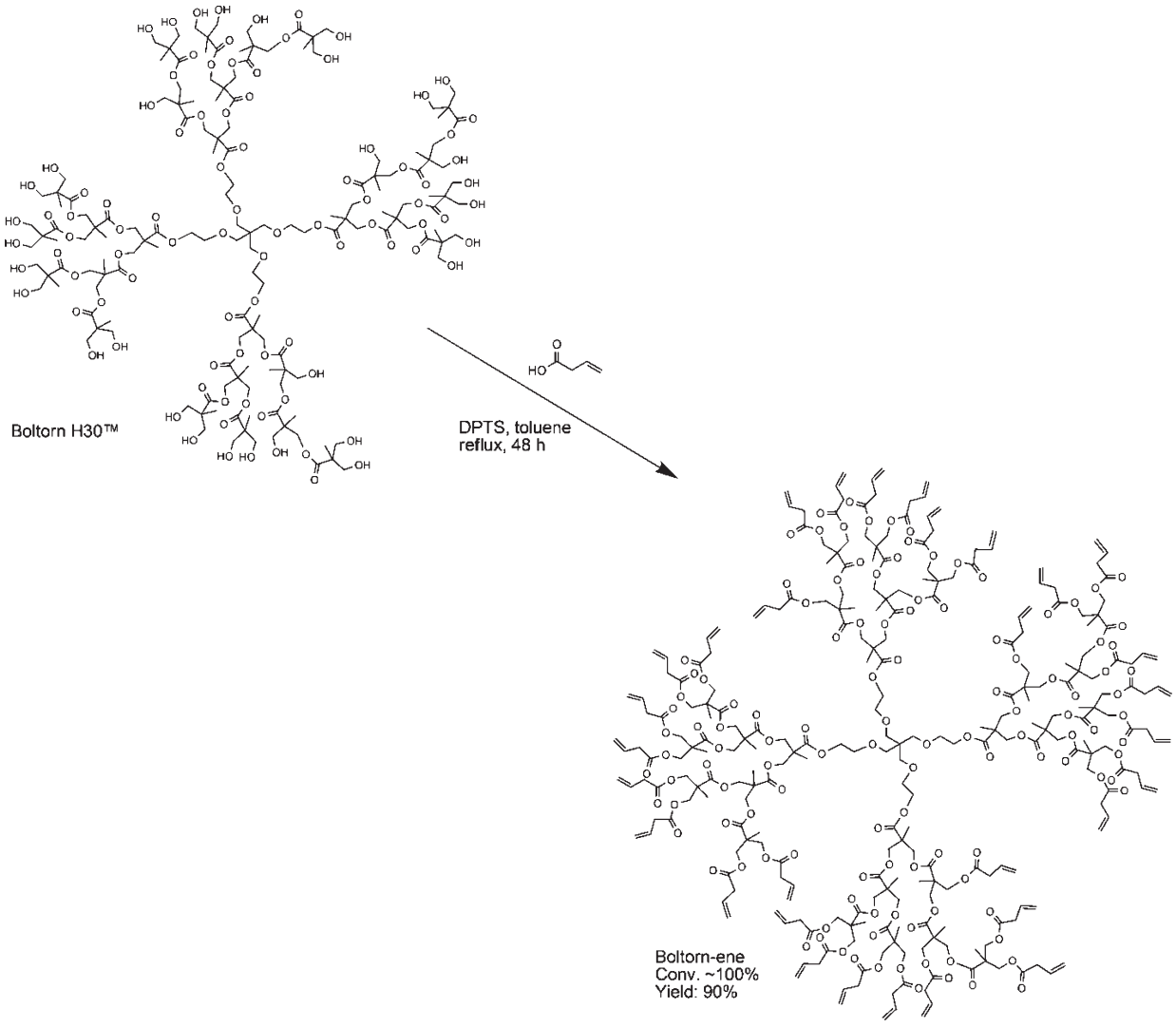

compartments of quadriperm dishes (Greiner) each containing a test surface. After 1 h in darkness at *ca.* 20 °C, the slides were gently washed in seawater to remove unsettled (i.e., motile) zoospores. Slides were fixed using 2.5% glutaraldehyde in seawater. The density of zoospores attached to the surface was counted on each of 3 replicates. Counts were made for 30 fields of view (each 0.17 mm^2), 1 mm apart across the central region of each slide, using a Zeiss epifluorescence microscope in conjunction with image analysis software (Imaging Associates Ltd.).[66]

Growth of Sporelings. Zoospores were settled on test samples and washed as described above. The spores germinated and developed into sporelings (young plants) over 10 days. Cultures were maintained in quadriperm dishes containing 10 mL of supplemented seawater medium that was changed every 2 days[67] and housed in an illuminated incubator (75 μmol m^{-2} s^{-1} incident irradiation).

Sporeling biomass was determined in situ by measuring the fluorescence of the chlorophyll contained within the cells in a Tecan fluorescence plate reader (excitation =430 nm, emission = 670 nm).[68] The biomass was quantified in terms of relative fluorescence units (RFU). The RFU value for each slide was the mean of 70 point fluorescence readings. The data are expressed as the mean RFU of 6 replicate slides; bars show SEM (standard error of the mean).

Attachment Strength of Sporelings. Strength of attachment of sporelings was assessed using an automated water jet that traversed the central region of each slide.[69] Individual slides of each treatment were exposed to a single impact pressures. The range of pressures used were selected to span from low to high biomass removal. The biomass remaining in the sprayed area was assessed using a fluorescence plate reader (as above). Percentage removal of biomass was calculated from readings taken before and after exposure to the water jet. The critical impact pressure to remove 50% of the biomass was determined from plots of percentage removal vs water impact pressure.[68] A polydimethylsiloxane elastomer (PDMSe; Silastic T2, Dow Corning, provided by Dr AB Brennan, University of Florida) was included in the assays as a standard fouling-release coating.[68]

RESULTS AND DISCUSSION

The highly alkenylated Boltorn-ene macromolecule was prepared in a manner similar to those previously published, wherein the dendritic polyester Boltorn H30 was esterified with 3-butenoic acid in the presence of a catalytic amount of DPTS (Scheme 1). Water was carefully removed from the Boltorn H30 prior to reaction via distillation. The mixture was allowed to

heat at reflux in anhydrous toluene for two days producing Boltorn-ene, **1**, as a thick clear oil in high yield and quantitative conversion. ^{1}H NMR spectroscopy (Figure 1), ^{13}C NMR spectroscopy and gel permeation chromatography (GPC) (see the Supporting Information, Figures S1 and S2, respectively) supported that the desired product was synthesized in high purity. The oil was readily prepared and stored in plastic syringes at 4 °C in order to minimize side reactions between the alkenes and atmospheric oxygen. Because of the low T_g of the polymer, the syringes acted as an ideal dispensing tool for the incorporation of Boltorn-ene into cross-linked coatings formulations with PEG and PETMP.

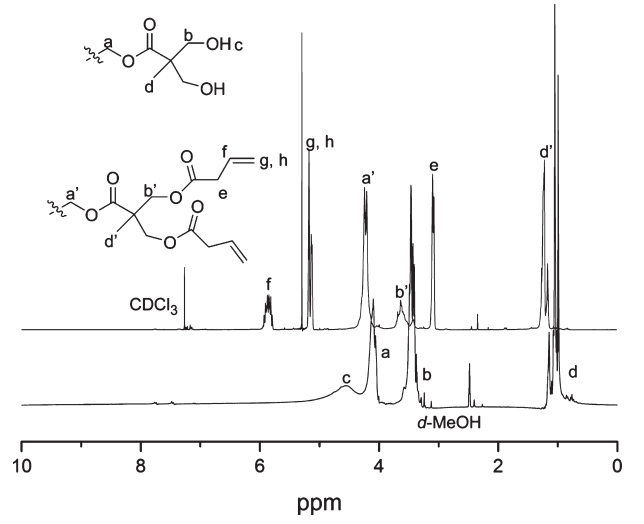

Figure 1. ^{1}H NMR spectra (300 MHz) of Boltorn H30 (*d*-MeOH, lower) and esterified Boltorn-ene ($CDCl_3$, upper).

A matrix approach was used for the preparation of cross-linked Boltorn-PEG-PETMP networks to ascertain to what extent the PEG and the PETMP contributed to the thermal, mechanical and surface properties of the materials. A 4 × 5 array of samples was prepared at constant Boltorn-ene weight, with four PEG weight percentages (0, 5, 15, and 25 wt % of the Boltorn-ene weight, corresponding to series A, B, C, and D, respectively) and five thiol concentrations (0, 0.25, 0.50, 0.75, and 1.0 equiv of SH of the PETMP cross-linker per eq alkene of Boltorn-ene molecule, corresponding to series 1, 2, 3, 4, and 5, respectively). For example, C3 would refer to a Boltorn-PEG-PETMP coating containing 15 wt % PEG and 0.50 equiv of SH/ene PETMP (Scheme 2). The photoinitiator, 1-hydroxycyclohexylphenyl ketone, was added at 5 wt % (w/w% of total solids), and the mixtures were dissolved in 1,4-dioxane to ensure complete homogeneity during mixing and pregel dispersion. The pregel solutions appeared to be shelf-stable at room temperature for several hours with no signs of premature cross-linking or gelation. The pregel solutions were syringed onto freshly prepared vinyl-trimethoxysilyl-modified glass slides to provide covalent

Scheme 2. Photoinitiated Curing of Boltorn-PEG-PETMP Copolymer Networks at Varying PEG and PETMP Concentrations

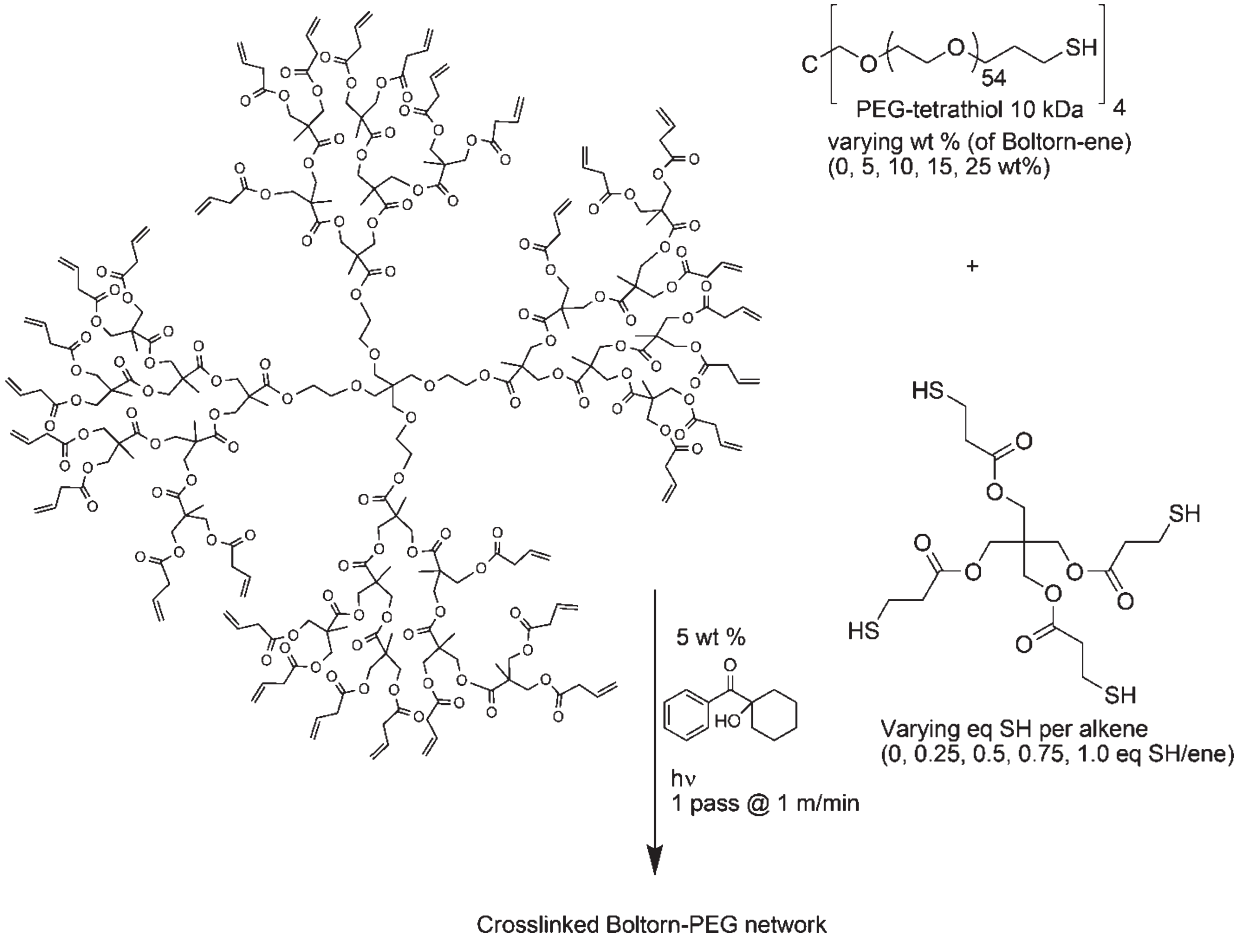

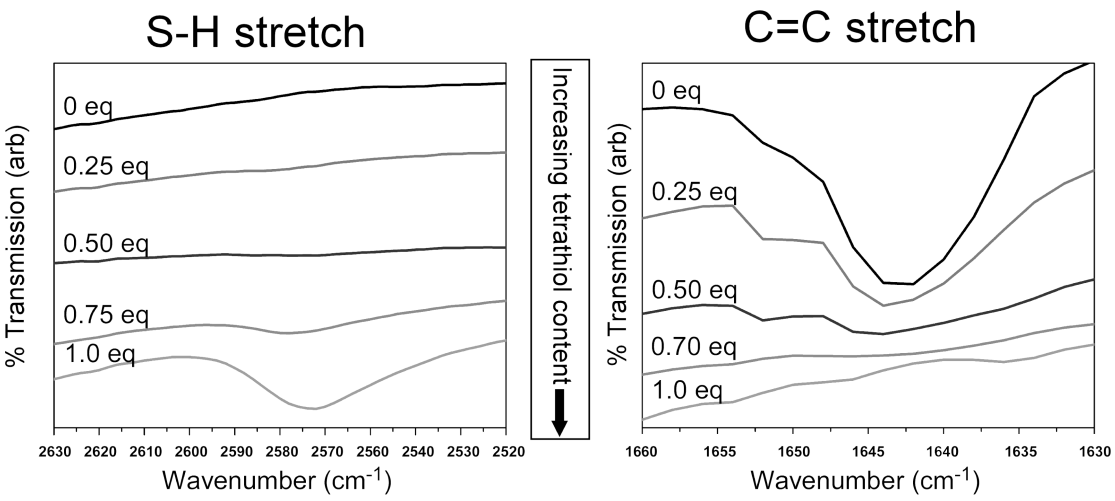

Figure 2. Example of IR spectroscopy results for Boltorn-PEG5-PETMP films ("B series") at varying PETMP concentrations.

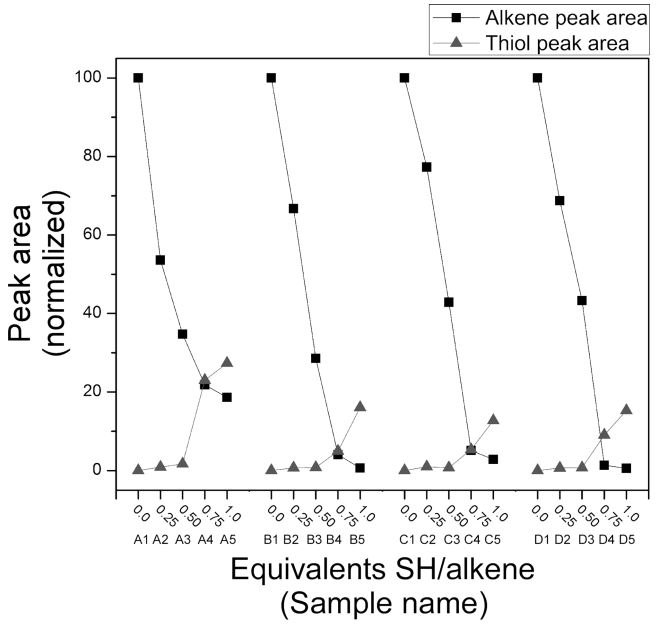

Figure 3. Normalized peak area of S−H and C═C stretches across the Boltorn-PEG-PETMP series.

cross-links between the glass and the Boltorn-PEG-PETMP film, whereby free thiols incorporated in the network underwent reaction with the surface vinyl silane groups. After the solutions were cast on the modified glass slides, a 20 min delay allowed for excess solvent to evaporate leaving a thickened optically transparent pregel mixture. The coated slides were then passed through a Fusion UV 300S conveyor system equipped with an H bulb (600 W) at a speed of 1 m/min for a single pass. This overall process produced transparent, copolymer networks in the range of 100−500 μm thick covalently bound to the glass substrate. The coated slides were then evaluated closely for defects, such as incomplete slide coverage, cracking or uneven thickness, prior to further characterization studies.

Infrared spectroscopy was used to determine the relative amounts of thiol and alkene that remained in the final cross-linked products. This analysis was accomplished by cross-linking a drop of pregel solution on a NaCl plate, followed by collection of the IR spectrum. An example of the relevant IR regions can be seen in Figure 2, which shows the "B series" as a typical example of the Boltorn-PEG-PETMP coatings. The specific bands highlighted are the S−H stretch at ca. 2570 cm^{-1} and the C═C stretch at ca. 1645 cm^{-1}. The C−S stretch and S−S stretch are not easily observed and cannot serve as an adequate measure for the formation of cross-linked networks. As PETMP concentration was increased, the band in the IR spectra corresponding to the S−H bond intensified providing evidence of excess or unconsumed thiol groups in the network, while the stretch associated with the C═C bond decreased rapidly as the groups were consumed. There appeared to be complete consumption of both functional groups at approximately 0.75 equiv of SH/ene PETMP concentration and an overabundance of thiol at 1.0 equiv of SH/ene. This deviation can be attributed to the limited accuracy of IR combined with a lack of ability to measure the full alkene concentration because of overlapping signals. Varying the PEG wt % did not affect the extent of reaction, quantified and evaluated by comparing peak areas across the series (Figure 3, series A vs. B vs. C vs. D), because the four thiol end groups of the PEG tetrathiol (4 SH/10 000 Da molecule) are dilute relative to the total thiol concentration provided by PETMP (4 SH/488 Da molecule) across all of the mixtures. It was observed that alkene consumption was relatively similar for each copolymer network composition, until 0.75 equiv SH/ene PETMP. At this ratio, samples with no PEG ("A series") appeared to reach reaction completion with approximately 10% of the free alkenes remaining in the bulk. An excess of thiol remained at a PETMP concentration of 1.0 equiv SH/ene, which could either be in the form of partially reacted or nonreacted PETMP trapped in the bulk; whichever the form, an odor from PETMP was noted.

The thermal transition temperatures and thermal stabilities were evaluated by differential scanning calorimetry and thermogravimetric analysis, respectively, after collection of samples by scraping from the glass substrates. The T_g values increased by approximately 20 °C as the PETMP concentration was increased from 0.0 to 1.0 equiv of SH/ene, regardless of PEG wt %, because of higher degrees of cross-linking achieved (Table 1, see Figures S6 and S7 in the Supporting Information). However, there was an inverse relationship with PEG wt %, where the T_g decreased by as much as 30 °C (depending on PETMP concentration) as

Table 1. Summary of the Thermomechanical Properties, Elemental Analysis and Contact Angle for the Boltorn-PEG-PETMP Films and Components. Data for the Antifouling (AF) Series Can Be Found in the Supporting Information, Table S1

			thermomechanical data		elemental analysis			contact angle		
sample	PEG (wt %)	thiol content (eq SH/ene)	T_g (°C)	T_{decomp} (°C)	carbon (%)	hydrogen (%)	sulfur (%)	advancing, θ_a (deg)	receding, θ_r (deg)	hysteresis, $\theta_a - \theta_r$ (deg)
Boltorn-ene			−37	427	57.21	6.51				
PEG-SH_4			n/a (T_m = 54)	396	52.19	8.78	2.15			
PETMP			n/a	373	41.88	5.77	26.34			
A1	0	0	−17	424	54.44	6.65	0.00	60 ± 4	49 ± 1	11
A2	0	0.25	−14	419	55.75	6.48	3.80	74 ± 4	60 ± 1	14
A3	0	0.50	15	423	53.81	6.46	6.39	77 ± 2	60 ± 2	17
A4	0	0.75	18	413	52.70	6.45	8.42	79 ± 2	64 ± 2	15
A5	0	1.00	16	428	51.16	6.33	9.91	65 ± 2	51 ± 1	14
B1	5	0	−21	412	57.63	6.82	0.19	69 ± 3	50 ± 2	19
B2	5	0.25	−15	403	55.36	6.64	4.08	71 ± 1	49 ± 6	21
B3	5	0.50	10	384	53.72	6.60	6.94	73 ± 2	52 ± 5	21
B4	5	0.75	21	384	52.84	6.51	8.64	80 ± 2	63 ± 4	17
B5	5	1.00	23	381	51.79	6.31	10.05	70 ± 1	52 ± 2	18
C1	15	0	−29	397	56.98	6.86	0.36	58 ± 3	41 ± 3	17
C2	15	0.25	−16	388	55.26	6.77	3.47	76 ± 2	59 ± 3	15
C3	15	0.50	−4	378	53.68	6.39	6.04	86 ± 3	69 ± 3	17
C4	15	0.75	−10	376	52.62	6.59	8.12	76 ± 2	61 ± 2	15
C5	15	1.00	−10	373	51.84	6.44	10.51	19 ± 3	4 ± 2	15
D1	25	0	−23	386	56.61	7.00	0.49	80 ± 3	62 ± 1	18
D2	25	0.25	−22	373	54.54	6.81	3.50	72 ± 3	52 ± 2	20
D3	25	0.50	−15	357	53.47	6.62	5.84	83 ± 2	65 ± 3	18
D4	25	0.75	−9	367	52.66	6.45	7.77	74 ± 3	59 ± 1	15
D5	25	1.00	−8	362	51.00	6.39	13.44	10 ± 1	3 ± 2	7

PEG content was increased. The PEG T_m transition (see Figure S6 in the Supporting Information), was not observed in any of the Boltorn-PEG-PETMP network DSC traces, potentially because of the restricted mobility of cross-linked or partially cross-linked PEG inhibiting crystallization. TGA analysis of the films (Table 1 and see Figure S8 in the Supporting Information) showed a decrease in the temperature at which the midpoint of degradation had occurred with increasing PEG and/or PETMP wt %, a consistent observation considering that both components have slightly lower peak degradation temperatures than that of the parent Boltorn-ene dendrimer (see Figure S9 in the Supporting Information).

The cross-linked copolymer network surfaces were examined using contact angle analysis and AFM. Interestingly, regardless of PEG wt %, both advancing and receding contact angle values of water appeared to increase until 0.50−0.75 equiv of SH/ene, followed by a decline at 1.0 equiv of SH/ene. This increase can be attributed to increased cross-linking density, in addition to increased hydrophobicity from the backbone of the PETMP cross-linker. The decline at 1.0 equiv of SH/ene is likely due to the presence of an excess of noncross-linked/partially cross-linked PETMP, presenting excess hydrophilic thiol groups throughout the polymer bulk and surface. There are a few trends that were observed from the initial static contact angles (Table 1) and time-dependent static contact angles, measured over a 3 h time period (see Figure S10 in the Supporting Information). Depending on PEG wt % and PETMP concentration, the contact angle typically decreased over time. Contact angle hysteresis did not seem to change across any of the coating formulations of PEG or PETMP wt %, and was typically between 15 and 20°. Visualization of the surface with AFM allowed for investigation into surface roughness. The features were relatively smooth at with 0 and 5 PEG wt % but gained nanoscopic roughness at higher PEG wt % (Figure 4).

The mechanical properties of Boltorn-PEG-PETMP free-standing thin films were measured using tensile testing, in the dry or water swollen states, using a Hencky strain of 0.01 s^{-1}. The contour plot of Young's modulus, E_{dry}, as a function of PEG wt % and PETMP concentration (Figure 5 and Figure S12 in the Supporting Information) revealed a strong dependence of thiol content on modulus, with maxima found at approximately 0.50−0.75 equiv of SH/ene cross-linker concentration for all PEG wt %. The decrease in modulus observed on going from 0.75 eq SH/ene to 1.00 eq SH/ene is likely to be a result of excess cross-linker, as verified by IR spectroscopy (vide supra), partially plasticizing the cross-linked film. There appeared to be a minor effect with respect to the PEG, in that an increase in PEG wt % gave a slight decrease in modulus. Similar trends with PEG and PETMP wt % were observed for the ultimate tensile strength (σ_{UTS}). The failure strains for the Boltorn-PEG-PETMP films were low, between approximately 10−30%. Exceptions were the films having no PETMP (A1, B1, C1, and D1), where the elongation was much higher, 30−80%, because of the low T_g and subsequent flexibility of the films. A summary of measured modulus values, ultimate tensile strengths and percent elongations have been compiled (Table 2). There did not appear to be

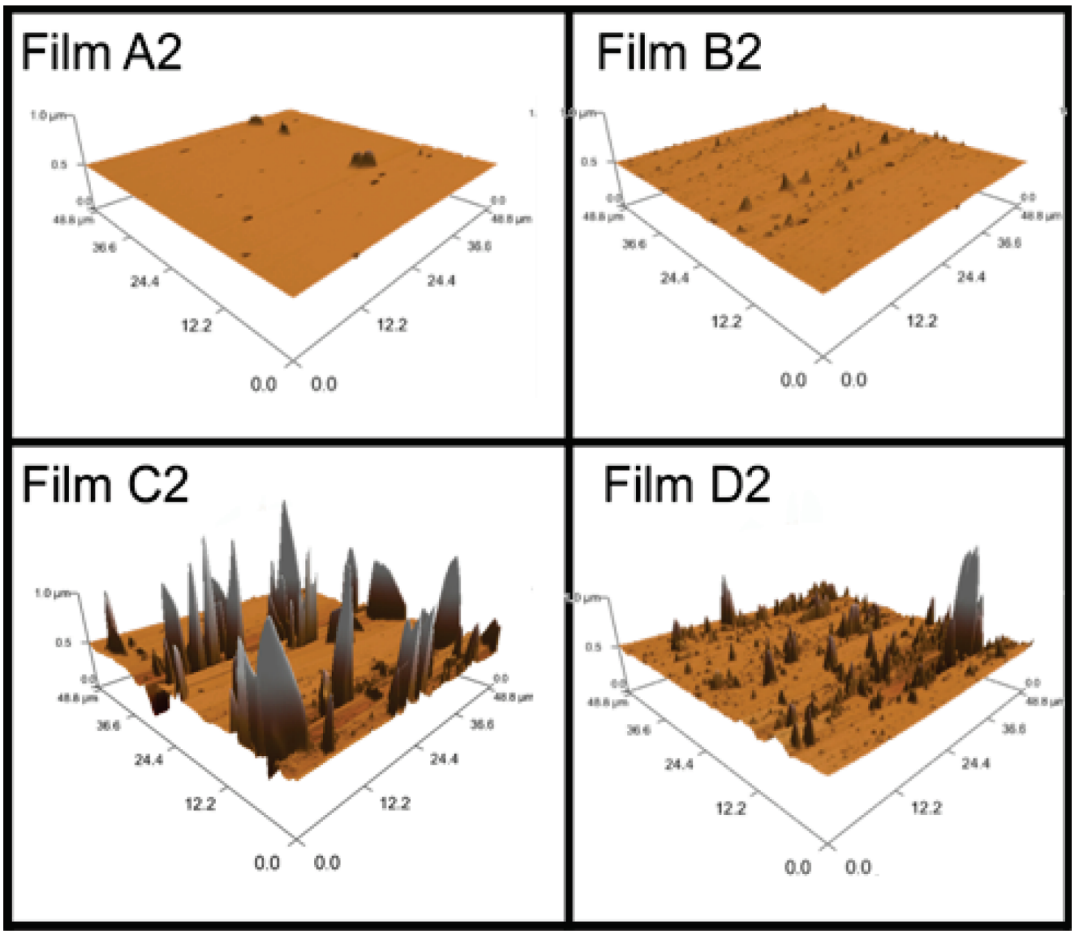

Figure 4. AFM images of Boltorn-PEG-PETMP networks at 0 PEG wt % (upper left, rms roughness = 8 nm), 5 PEG wt % (upper right, rms roughness = 8 nm), 15 PEG wt % (lower left, rms roughness = 115 nm) and 25 PEG wt % (lower right, rms roughness = 67 nm) in the dry state [50 × 50 μm^2 scan size; z axis = 1.0 μm].

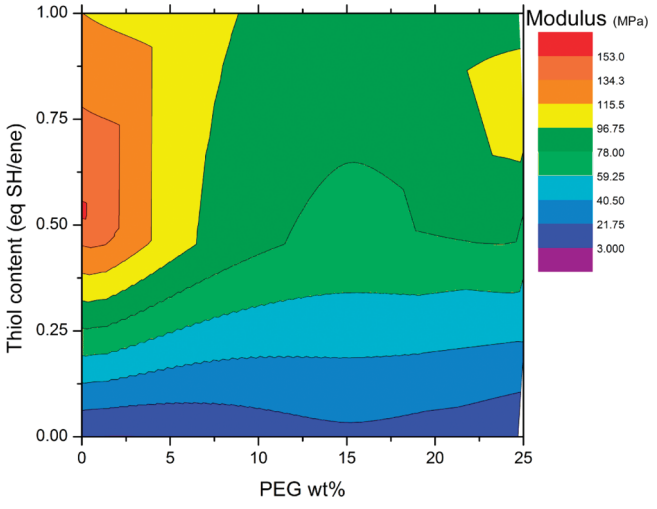

Figure 5. Contour plot of Young's modulus data for the Boltorn-PEG-PETMP series as a function of PEG wt % (x axis) and PETMP concentration (y axis).

as large of a disparity between the Young's modulus of wet and dry Boltorn-PEG-PETMP films as had been observed with the HBFP-PEG series materials;[55] however, there is a statistically significant difference in ultimate tensile strength (Figure 6). At a constant 0.25 equiv of SH/ene cross-linker concentration (films A2, B2, C2, and D2), the modulus values for wet and dry films were similar, with the exception of C2. C2 showed a decrease in modulus between the dry to wet state, whereas the ultimate tensile strength actually increased when wet. Additional tensile tests were performed for the remainder of the "C series" (C1, C3, C4, and C5; see Figure S13 in the Supporting Information), for which similar trends were observed with the modulus, but not for the ultimate tensile strength.

Efforts were then focused on a narrower range of coatings formulations having a broader range of PEG wt % for biofouling testing. A detailed series of Boltorn-PEG-PETMP films was produced at a low, constant PETMP concentration of 0.25 equiv SH/ene (16 wt %) and varying PEG wt % (0, 5, 10, 15, 20, 25, 30, and 35 wt %). These coatings were tested against a soft fouling marine alga and assessed through two experiments—spore settlement (attachment) and the strength of attachment of sporelings (release). The strength of attachment was determined by exposing the surfaces to a range of impact pressures generated by a water jet. Spore settlement densities were low on all of the amphiphilic coatings compared to that on a polydimethylsiloxane (PDMSe) standard (Figure 7). Although spore density was low, it increased with increases in PEG content. One-way analysis of variance on spore density for the amphiphilic samples alone

Table 2. Summary of the Mechanical Properties for the Boltorn-PEG-PETMP Films in Both Dry and Wet Conditions

			before swelling in water			after swelling in water		
sample	PEG (wt %)	thiol content (equiv of SH/ene)	ultimate tensile strength (σ_{UTS}, MPa)	failure strain ε_f (%)	E_{dry} (MPa)	ultimate tensile strength σ_{UTS} (MPa)	failure strain ε_f (%)	E_{wet} (MPa)
A1	0	0	141 ± 36	48 ± 8	3 ± 1			
A2	0	0.25	791 ± 205	19 ± 6	73 ± 8	1095 ± 293	26 ± 3	70 ± 10
A3	0	0.50	2811 ± 679	34 ± 6	153 ± 18			
A4	0	0.75	2096 ± 352	38 ± 11	149 ± 7			
A5	0	1.00	1922 ± 477	27 ± 7	119 ± 10			
B1	5	0	135 ± 51	32 ± 20	4 ± 1			
B2	5	0.25	532 ± 155	13 ± 4	60 ± 3	953 ± 137	21 ± 2	64 ± 6
B3	5	0.50	2313 ± 374	45 ± 11	112 ± 7			
B4	5	0.75	2099 ± 437	32 ± 10	121 ± 18			
B5	5	1.00	1281 ± 357	20 ± 10	106 ± 7			
C1	15	0	558 ± 213	78 ± 39	18 ± 5	71 ± 17	38 ± 13	3 ± 1
C2	15	0.25	541 ± 173	14 ± 5	53 ± 2	853 ± 308	29 ± 13	38 ± 2
C3	15	0.50	689 ± 107	11 ± 1	77 ± 8	789 ± 496	13 ± 11	63 ± 20
C4	15	0.75	1192 ± 455	19 ± 8	96 ± 10	521 ± 168	11 ± 2	84 ± 20
C5	15	1.00	652 ± 251	11 ± 2	87 ± 9	1261 ± 154	27 ± 3	85 ± 14
D1	25	0	208 ± 49	66 ± 24	4 ± 2			
D2	25	0.25	352 ± 40	11 ± 1	45 ± 4	461 ± 198	14 ± 5	47 ± 5
D3	25	0.50	1330 ± 297	27 ± 8	84 ± 8			
D4	25	0.75	1634 ± 124	23 ± 2	105 ± 5			
D5	25	1.00	1592 ± 144	30 ± 5	93 ± 6			

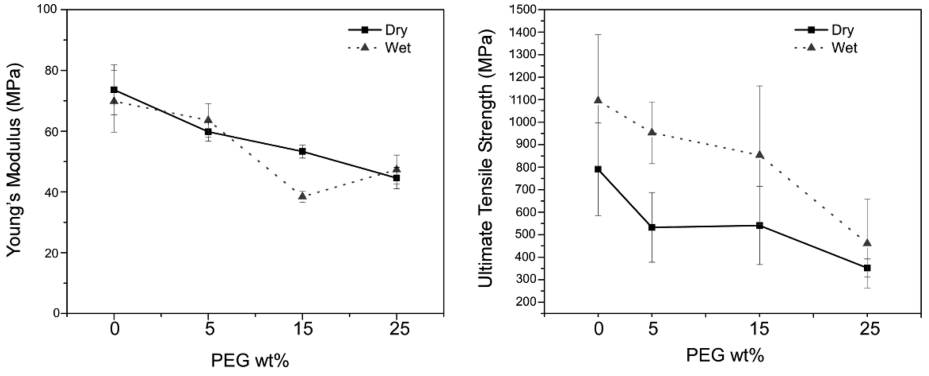

Figure 6. Young's modulus (left) and ultimate tensile strength (right) for the "2 series" (A2, B2, C2, and D2) as measured dry and wetted for 7 days in artificial seawater.

showed there were significant differences between the samples ($F_{7,712} = 80$, $P < 0.05$). A Tukey test showed that the settlement densities on the majority of coatings were significantly different to each other, confirming the trend of increasing settlement density with increasing PEG content. Because of the increase in surface roughness with increasing PEG wt %, it is possible that the settlement increases as a function of PEG were directly due to the loss of a smooth, highly hydrophilic surface. Self-assembled monolayers formed from PEG inhibit the settlement of spores[17] and studies on PEG-containing systems have generally shown the opposite trend, i.e., settlement densities decreased with increasing PEG content.[70] For the PEG-SAMs, the inhibition of settlement has been attributed to the increased hydrophilicity and subsequent hydration of the coating and for amphiphilic coatings, surface restructuring following immersion produced changes to surface nanostructure,[71] possibly making it more difficult for spores to "detect" and adhere to the surface. It is also possible that the increased spore settlement density could be due to residual surface thiols on the PEG termini, which could undergo disulfide-based covalent conjugation with cysteines of spore proteins. The DACM-thiol fluorescence experiment showed that there was a minor amount of surface thiols (~5−10 fluorescent %) present in the AF film series (Figure 8), which could contribute to the fouling character of the Boltorn-PEG-PETMP films. Sporeling biomass was evaluated on all the coatings after 10 days of growth. Sporelings grew normally on all of the samples with no signs of toxicity, although as expected form the low density of settled spores, the amount of biomass was lower on the amphiphilic cross-linked network samples than on the PDMSe standard (see Figure S14 in the Supporting Information).

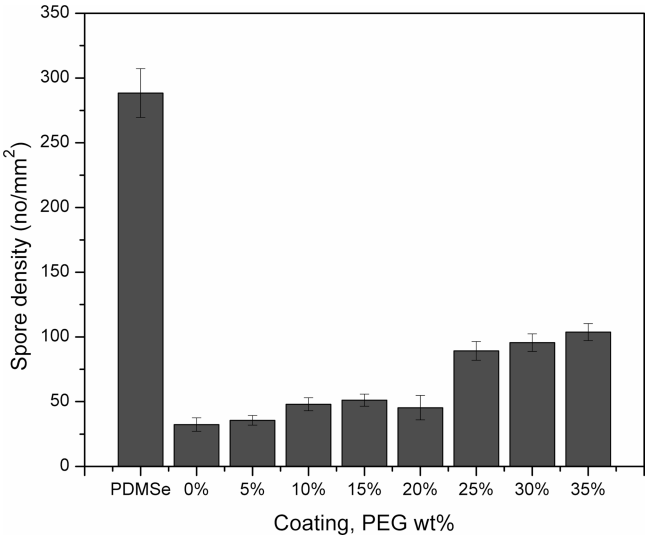

Figure 7. Settlement density of spores of *Ulva* on amphiphilic coatings after 1 h settlement. The density of spores on Nexterion glass (Schott) was 767 spores mm^{-2}. Each point is the mean from 90 counts on 3 replicate slides. Bars show 95% confidence limits.

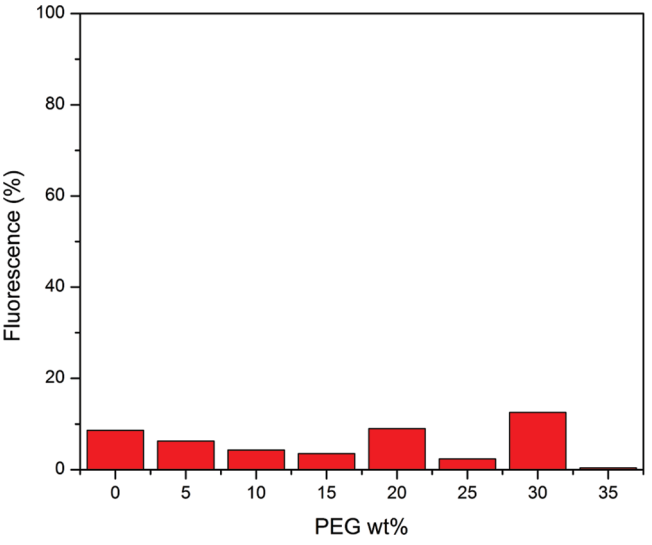

Figure 8. Surface DACM-thiol fluorescence of the antifouling coating series.

Table 3. Critical Surface Pressures for 50% removal of Sporeling Biofilms Derived from Curves in Figure S17 and Percent Removal of Sporeling Biofilms at the Single Water Pressure of 64 kPa[a]

label (PEG wt %)[b]	critical water pressure to remove 50% of biomass (kPa)	% removal at pressure of 64 kPa
PDMSe	50	75
15	~93	57
10	~112	45
5	184	18
0	184	8

[a] Samples are listed in order of ease of removal. [b] The coatings with PEG content greater than 15% delaminated and were not tested.

Because of delamination issues with higher PEGylated coatings, sporeling strength of attachment was measured only for the 0, 5, 10, and 15 PEG wt % coatings. Sporelings were attached more strongly on all of the coatings than on the PDMSe standard, however, ease of removal increased with increasing PEG content, where the highest removal was observed from the 15 PEG wt % coating regardless of pressure. The critical water pressures to remove 50% of the biofilms are shown in Table 3 and Figure S15 in the Supporting Information.

CONCLUSIONS

A series of Boltorn-PEG-PETMP films was prepared by the photoinitiated thiol−ene cross-linking of Boltorn-ene in the presence of both 4-armed PEG tetrathiol and PETMP. The properties of these complex, amphiphilic copolymer networks, including T_g, Young's modulus, contact angle, and surface roughness were dependent on the PEG and PETMP concentrations. Identification of the optimal amount of PETMP allowed for investigation of Boltorn-PEG-PETMP coatings prepared with 0.25 equiv of SH/ene PETMP concentration at varying PEG concentrations for resistance against *Ulva* spore settlement. These antibiofouling data will guide further studies to develop the Boltorn-PEG-PETMP system as a low cost, environmentally benign antibiofouling coating.

ASSOCIATED CONTENT

Supporting Information. ^{13}C NMR spectrum and GPC chromatogram for Boltorn-ene, extensive experimental procedures for all Boltorn-PEG-PETMP networks, IR spectra, DSC and TGA traces, dynamic water contact angle data, 2D modulus plots, tensile data contour plot, "C series" modulus and ultimate tensile strength plots, typical growth for algae sporelings on films and water jet removal graph for the films. This material is available free of charge via the Internet at http://pubs.acs.org.

AUTHOR INFORMATION

Corresponding Author

*Tel. (979) 845-4077. Fax (979) 862-1137. E-mail: wooley@chem.tamu.edu.

ACKNOWLEDGMENT

The authors thank Perstorp for the sample of Boltorn H30. This research is based on work supported by the Office of Naval Research under Grants N00014-08-1-0398 and N00014-10-1-0527 (K.W.) and N00014-08-1-0010 (J.A.C./M.E.C.). Assistant Professor fellowship from the Knut and Alice Wallenberg Foundation (to A.M.N.), as well as financial support from Åke Wibergs foundation, Karolinska Insitutet, The Swedish Medical Nanoscience Center, and from the Swedish Research Council 2009-3259, are also gratefully acknowledged.

REFERENCES

(1) Yebra, D. M.; Kiil, S.; Dam-Johansen, K. *Prog. Org. Coat.* **2004**, *50*, 75–104.

(2) Chambers, L. D.; Stokes, K. R.; Walsh, F. C.; Wood, R. J. K. *Surf. Coat. Technol.* **2006**, *201*, 3642–3652.

(3) Howell, D.; Behrends, B. In *Biofouling*; Duerr, S., Thomason, J. C., Eds.; John Wiley & Sons: New York, 2010; pp 226−251.

(4) Krishnan, S.; Ayothi, R.; Hexemer, A.; Finlay, J. A.; Sohn, K. E.; Perry, R.; Ober, C. K.; Kramer, E. J.; Callow, M. E.; Callow, J. A.; Fischer, D. A. *Langmuir* **2006**, *22*, 5075–5086.
(5) Bartels, J. W.; Cheng, C.; Powell, K. T.; Xu, J. Q.; Wooley, K. L. *Macromol. Chem. Phys.* **2007**, *208*, 1676–1687.
(6) Gudipati, C. S.; Finlay, J. A.; Callow, J. A.; Callow, M. E.; Wooley, K. L. *Langmuir* **2005**, *21*, 3044–3053.
(7) Yarbrough, J. C.; Rolland, J. P.; DeSimone, J. M.; Callow, M. E.; Finlay, J. A.; Callow, J. A. *Macromolecules* **2006**, *39*, 2521–2528.
(8) Youngblood, J. P.; Andruzzi, L.; Ober, C. K.; Hexemer, A.; Kramer, E. J.; Callow, J. A.; Finlay, J. A.; Callow, M. E. *Biofouling* **2003**, *19*, 91–98.
(9) Aldred, N.; Clare, A. S. *Biofouling* **2008**, *24*, 351–363.
(10) Beigbeder, A.; Degee, P.; Conlan, S. L.; Mutton, R. J.; Clare, A. S.; Pettitt, M. E.; Callow, M. E.; Callow, J. A.; Dubois, P. *Biofouling* **2008**, *24*, 291–302.
(11) Majumdar, P.; Lee, E.; Patel, N.; Ward, K.; Stafslien, S. J.; Daniels, J.; Boudjouk, P.; Callow, M. E.; Callow, J. A.; Thompson, S. E. M. *Biofouling* **2008**, *24*, 185–200.
(12) Marabotti, I.; Morelli, A.; Orsini, L. M.; Martinelli, E.; Galli, G.; Chiellini, E.; Lien, E. M.; Pettitt, M. E.; Callow, J. A.; Conlan, S. L.; Mutton, R. J.; Clare, A. S.; Kocijan, A.; Donik, C.; Jenko, M. *Biofouling* **2009**, *25*, 481–493.
(13) McMaster, D. M.; Bennett, S. M.; Tang, Y.; Finlay, J. A.; Kowalke, G. L.; Nedved, B.; Bright, S. M.; Callow, M. E.; Callow, J. A.; Wendt, D. E.; Hadfield, M. G.; Detty, M. R. *Biofouling* **2009**, *25*, 21–33.
(14) Li, G. Z.; Xue, H.; Gao, C. L.; Zhang, F. B.; Jiang, S. Y. *Macromolecules* **2010**, *43*, 14–16.
(15) Yang, W.; Zhang, L.; Wang, S. L.; White, A. D.; Jiang, S. Y. *Biomaterials* **2009**, *30*, 5617–5621.
(16) Zhang, Z.; Finlay, J. A.; Wang, L. F.; Gao, Y.; Callow, J. A.; Callow, M. E.; Jiang, S. Y. *Langmuir* **2009**, *25*, 13516–13521.
(17) Schilp, S.; Rosenhahn, A.; Pettitt, M. E.; Bowen, J.; Callow, M. E.; Callow, J. A.; Grunze, M. *Langmuir* **2009**, *25*, 10077–100082.
(18) Unsworth, L. D.; Sheardown, H.; Brash, J. L. *Langmuir* **2005**, *21*, 1036–1041.
(19) Rydholm, A. E.; Bowman, C. N.; Anseth, K. S. *Biomaterials* **2005**, *26*, 4495–4506.
(20) Ma, J.; Bartels, J. W.; Li, Z.; Zhang, K.; Cheng, C.; Wooley, K. L. *Aust. J. Chem.* **2010**, *63*, 1159–1163.
(21) Grozea, C. M.; Walker, G. C. *Soft Matter* **2009**, *5*, 4088–4100.
(22) Magin, C. M.; Cooper, S. P.; Brennan, A. B. *Mater. Today* **2010**, *13*, 36–44.
(23) Park, D.; Weinman, C. J.; Finlay, J. A.; Fletcher, B. R.; Paik, M. Y.; Sundaram, H. S.; Dimitriou, M. D.; Sohn, K. E.; Callow, M. E.; Callow, J. A.; Handlin, D. L.; Willis, C. L.; Fischer, D. A.; Kramer, E. J.; Ober, C. K. *Langmuir* **2010**, *26*, 9772–9781.
(24) Webster, D. C.; Chisholm, B. J. In *Biofouling*; Duerr, S., Thomason, J. C., Eds.; John Wiley & Sons: New York, 2010; pp 366−387.
(25) Feng, S. J.; Wang, Q.; Gao, Y.; Huang, Y. G.; Qing, F. L. *J. Appl. Polym. Sci.* **2009**, *114*, 2071–2078.
(26) Brady, R. F.; Singer, I. L. *Biofouling* **2000**, *15*, 73–81.
(27) Genzer, J.; Efimenko, K. *Biofouling* **2006**, *22*, 339–360.
(28) Hoipkemeier-Wilson, L.; Schumacher, J.; Carman, M.; Gibson, A.; Feinberg, A.; Callow, M.; Finlay, J.; Callow, J.; Brennan, A. *Biofouling* **2004**, *20*, 53–63.
(29) Scardino, A. J.; Zhang, H.; Cookson, D. J.; Lamb, R. N.; de Nys, R. *Biofouling* **2009**, *25*, 757–767.
(30) Killops, K. L.; Campos, L. M.; Hawker, C. J. *J. Am. Chem. Soc.* **2008**, *130*, 5062–5064.
(31) Kade, M. J.; Burke, D. J.; Hawker, C. J. *J. Polym. Sci., Part A: Polym. Chem.* **2010**, *48*, 743–750.
(32) Nilsson, C.; Malmstrom, E.; Johansson, M.; Trey, S. M. *J. Polym. Sci., Part A: Polym. Chem.* **2009**, *47*, 589–601.
(33) Nilsson, C.; Simpson, N.; Malkoch, M.; Johansson, M.; Malmstrom, E. *J. Polym. Sci., Part A: Polym. Chem.* **2008**, *46*, 1339–1348.
(34) Morgan, C. R.; Ketley, A. D. *J. Polym. Sci., Polym. Lett. Ed.* **1978**, *16*, 75–79.
(35) Morgan, C. R.; Magnotta, F.; Ketley, A. D. *J. Polym. Sci., Polym. Chem. Ed.* **1977**, *15*, 627–645.
(36) Ma, J.; Cheng, C.; Wooley, K. L. *Aust. J. Chem.* **2009**, *62*, 1507–1519.
(37) van Berkel, K. Y.; Hawker, C. J. *J. Polym. Sci., Part A: Polym. Chem.* **2010**, *48*, 1594–1606.
(38) Jones, M. W.; Mantovani, G.; Ryan, S. M.; Wang, X. X.; Brayden, D. J.; Haddleton, D. M. *Chem. Commun.* **2009**, 5272–5274.
(39) Chan, J. W.; Yu, B.; Hoyle, C. E.; Lowe, A. B. *Chem. Commun.* **2008**, 4959–4961.
(40) O'Brien, A. K.; Cramer, N. B.; Bowman, C. N. *J. Polym. Sci., Part A: Polym. Chem.* **2006**, *44*, 2007–2014.
(41) Cramer, N. B.; Scott, J. P.; Bowman, C. N. *Macromolecules* **2002**, *35*, 5361–5365.
(42) Hoyle, C. E.; Lee, T. Y.; Roper, T. *J. Polym. Sci., Part A: Polym. Chem.* **2004**, *42*, 5301–5338.
(43) Ihre, H.; Johansson, M.; Malström, E.; Hult, A. In *Advances in Dendritic Macromolecules*; Newkome, G. R., Ed.; JAI Press: Greenwich, CT, 1996; Vol. 3, pp 1−25.
(44) Mespouille, L.; Hedrick, J. L.; Dubois, P. *Soft Matter* **2009**, *5*, 4878–4892.
(45) Campos, L. M.; Meinel, I.; Guino, R. G.; Schierhorn, M.; Gupta, N.; Stucky, G. D.; Hawker, C. J. *Adv. Mater.* **2008**, *20*, 3728–3733.
(46) Hagberg, E. C.; Malkoch, M.; Ling, Y. B.; Hawker, C. J.; Carter, K. R. *Nano Lett.* **2007**, *7*, 233–237.
(47) Roper, T. M.; Kwee, T.; Lee, T. Y.; Guymon, C. A.; Hoyle, C. E. *Polymer* **2004**, *45*, 2921–2929.
(48) Guenthner, A. J.; Hess, D. M.; Cash, J. J. *Polymer* **2008**, *49*, 5533–5540.
(49) Lu, H.; Carioscia, J. A.; Stansbury, J. W.; Bowman, C. N. *Dent. Mater.* **2005**, *21*, 1129–1136.
(50) Lundberg, P.; Bruin, A.; Klijnstra, J. W.; Nyström, A. M.; Johansson, M.; Malkoch, M.; Hult, A. *ACS Appl. Mater. Interfaces* **2010**, *2*, 903–912.
(51) Hu, Z. K.; Finlay, J. A.; Chen, L.; Betts, D. E.; Hillmyer, M. A.; Callow, M. E.; Callow, J. A.; DeSimone, J. M. *Macromolecules* **2009**, *42*, 6999–7007.
(52) Anseth, K. S.; Metters, A. T.; Bryant, S. J.; Martens, P. J.; Elisseeff, J. H.; Bowman, C. N. *J. Controlled Release* **2002**, *78*, 199–209.
(53) Gudipati, C. S.; Greenlief, C. M.; Johnson, J. A.; Prayongpan, P.; Wooley, K. L. *J. Polym. Sci., Part A: Polym. Chem.* **2004**, *42*, 6193–6208.
(54) Xu, J.; Bartels, J. W.; Bohnsack, D. A.; Tseng, T.-C.; Mackay, M. E.; Wooley, K. L. *Adv. Funct. Mater.* **2008**, *18*, 2733–2744.
(55) Xu, J. Q.; Bohnsack, D. A.; Mackay, M. E.; Wooley, K. L. *J. Am. Chem. Soc.* **2007**, *129*, 506–507.
(56) Brown, G. O.; Bergquist, C.; Ferm, P.; Wooley, K. L. *J. Am. Chem. Soc.* **2005**, *127*, 11238–11239.
(57) Fu, Q.; Liu, J.; Shi, W. *Prog. Org. Coat.* **2008**, *63*, 100–109.
(58) Schmidt, L. E.; Schmah, D.; Leterrier, Y.; Manson, J. A. E. *Rheol. Acta* **2007**, *46*, 693–701.
(59) Fu, Q.; Cheng, L.; Zhang, Y.; Shi, W. *Polymer* **2008**, *49*, 4981–4988.
(60) Fogelström, L.; Antoni, P.; Malmström, E.; Hult, A. *Prog. Org. Coat.* **2006**, *55*, 284–290.
(61) Miao, H.; Cheng, L.; Shi, W. *Prog. Org. Coat.* **2009**, *65*, 71–76.
(62) Neumann, A. W.; Good, R. J. *J. Surf. Colloid Sci.* **1979**, *11*, 31–91.
(63) Haynes, R. K.; Katsifis, A.; Vonwiller, S. C. *Aust. J. Chem.* **1984**, *37*, 1571–1578.
(64) Moore, J. S.; Stupp, S. I. *Macromolecules* **1990**, *23*, 65–70.
(65) Callow, M. E.; Callow, J. A.; Pickett-Heaps, J. D.; Wetherbee, R. *J. Phycol.* **1997**, *33*, 938–947.
(66) Callow, M. E.; Jennings, A. R.; Brennan, A. B.; Seegert, C. E.; Gibson, A.; Wilson, L.; Feinberg, A.; Baney, R.; Callow, J. A. *Biofouling* **2002**, *18*, 237–245.

(67) Starr, R. C.; Zeikus, J. A. *J. Phycol.* **1987**, *23*, 1–47.
(68) Finlay, J. A.; Fletcher, B. R.; Callow, M. E.; Callow, J. A. *Biofouling* **2008**, *24*, 219–225.
(69) Finlay, J. A.; Callow, M. E.; Schultz, M. P.; Swain, G. W.; Callow, J. A. *Biofouling* **2002**, *18*, 251–256.
(70) Park, D.; Weinman, C. J.; Finlay, J. A.; Fletcher, B. R.; Paik, M. Y.; Sundaram, H. S.; Dimitriou, M.; Sohn, K. E.; Callow, M. E.; Callow, J. A.; Handlin, D. L.; Willis, C. L.; Fischer, D. A.; Kramer, E. J.; Ober, C. K. *Langmuir* **2010**, *26*, 9772–9781.
(71) Martinelli, E.; Agostini, S.; Galli, G.; Chiellini, E.; Glisenti, A.; Pettitt, M. E.; Callow, M. E.; Callow, J. A.; Graf, K.; Bartels, F. W. *Langmuir* **2008**, *24*, 13138–13147.